JOURNAL OF SOLID STATE CHEMISTRY 65, 13–26 (1986)

Structural Studies of Cs–K–Bi Mixed Chlorides Relation to the Crystal Structures of A_2BMX_6, A_3MX_6, and A_2MX_6

FARIDA BENACHENHOU, GAËTAN MAIRESSE,*
GUY NOWOGROCKI, AND DANIEL THOMAS

Laboratoire de Cristallochimie et Physicochimie du Solide (UA CNRS 452), Ecole Nationale Supérieure de Chimie, B.P. 108 59652 Villeneuve d'Ascq Cedex, France

Received February 18, 1986

The room-temperature crystal structures of Cs_3BiCl_6(I) and CsK_2BiCl_6(II) have been determined from X-ray single-crystal data. These compounds are both monoclinic, space group $C2/c$, with eight formula units per cell and cell parameters $a = 27.017(17)$, $b = 8.252(8)$, $c = 13.121(10)$ Å, $\beta = 99.70(11)°$ (I), $a = 25.653(13)$, $b = 7.799(5)$, $c = 12.874(9)$ Å, $\beta = 99.24(8)°$ (II). The crystal structures have been refined to final R values of 0.069(I) and 0.044(II) from 1706(I) and 2008(II) independent reflections and 93 variable parameters. The $BiCl_6$ octahedra are slightly distorted (average $d_{Bi-Cl} = 2.699$ Å) and the alkaline cations are coordinated with eleven or eight chlorine atoms. These structures are better described using the notion of "layers of close-packed octahedra" and can therefore be easily compared with the A_2BMX_6 (elpasolite type), A_3MX_6 (cryolite type), and A_2MX_6 (K_2PtCl_6 type) crystal structures. In these compounds, the "layers" of isolated octahedral MX_6 entities (X = F, Cl, Br, O) define "tetrahedral" and "octahedral" holes, entirely or partially occupied by the A and/or B cations.

Introduction

Recent structural and physicochemical investigations of A_2BMCl_6 mixed chlorides (where A and B are alkaline metals and M a trivalent element) have disclosed ferroelastic-type phase transitions at low (*1*) and high (*2*) temperature, as well as distortions of the cubic elpasolite structure (*3*). In this last work, it was shown from powder diffraction data that for almost all compositions, the room-temperature phase is strongly distorted, as compared to the high-symmetry, high-temperature phase. Only in the case of the Cs_2KBiCl_6 composition is the ideal elpasolite structure retained down to room temperature.

The phase-transition diagram of the $Cs_{3-x}K_x BiCl_6$ ($0 \leq x \leq 3$) system has been recently reported (*4*). In the high-temperature region, a continuous solid solution with the cubic $Fm3m$ crystal structure extends throughout the whole system. Two ($x > 1$) or three ($x < 1$) phase transitions occur as the temperature is lowered (except for $x = 1$: Cs_2KBiCl_6 composition) (Fig. 1), some of these transitions probably being of the ferroelastic type (*4–6*). Cs_3BiCl_6 presents, at temperatures lower than $T_1 = 120°C$ (phase I), potential physical properties ac-

* To whom correspondence should be addressed.

0022-4596/86 $3.00

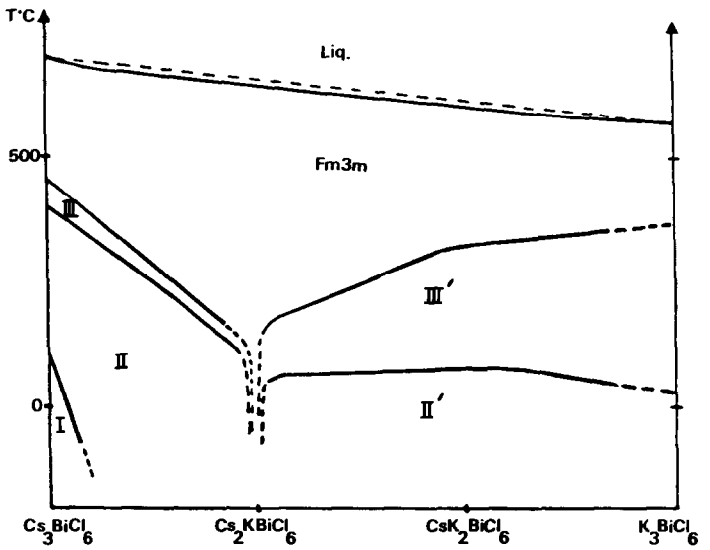

FIG. 1. Binary diagram Cs_3BiCl_6–K_3BiCl_6.

cording to the observed remanent polarization, although this phenomenon does not seem to have a ferroelectric origin (*6*).

The only available structural data on $Cs_{3-x}K_xBiCl_6$ phases deal with Cs_2KBiCl_6 (*3, 5*): this compound is isostructural with $Cs_2NaBiCl_6$, which was assigned cubic *Fm3m* symmetry from single-crystal data (*7*). Clearly, more work is needed to understand the evolution of the structures and to establish some structural relationships as the composition or temperature is changed. The present paper deals with the first aspect of this question: it describes the structures of crystals with compositions corresponding to $x = 0$ (phase I) and $x = 2$ (phase II'), which are stable at room temperature, and symmetrically located on each side of Cs_2KBiCl_6.

Experimental

A transport method was initially considered to take advantage of the large partial pressure of $BiCl_3$ at high temperature. Indeed, heating in a temperature gradient an evacuated sealed quartz tube containing mixture of chlorides led to the deposition of well shaped single crystals. Unfortunately, they stuck strongly to the quartz wall and could not be recovered without damage.

An alternative method was therefore used: slow cooling (5°C · hr^{-1}) of a small amount (~500 mg) of a mixture of chlorides, from the congruent melting point to the ambient temperature, resulted in a thin transparent layer, from which small flakes could be recovered. The selected samples were roughly triangular with maximum lengths of about 150 and 250 μm for Cs_3BiCl_6 and CsK_2BiCl_6, respectively.

Structure Determination

Preliminary investigations of Cs_3BiCl_6 and CsK_2BiCl_6 had led to the hypothesis of a triclinic $P\bar{1}$ unit cell (*5*), but the actual symmetry was proved to be *C*2/*c* from single-crystal studies (*hkl* with $h + k = 2n$ and *h*0*l* with $l = 2n$). X-Ray patterns and the diffractometer data indicated that the Cs_3BiCl_6 crystal was of poor quality: it was twinned and composed of two individuals

with slightly different orientations (about 0.1° in θ, χ, φ). This situation is probably due to ferroelastic transitions occurring during the cooling (*4*). Despite these troubles, we managed to collect the reflections from the bigger individual, which was almost twice the volume of the other one. In addition, some superstructure reflections have been detected on Weissenberg patterns; taking them into account led to doubling of the unit cell. However, in view of their very low intensity (which was never larger than 1.5 times their standard deviation), they were not included in the refinement process. With the CsK_2BiCl_6 single crystal, neither twinning nor superstructure reflections were observed.

Data collection was made using the Philips PW1100 four circle automated diffractometer of the "Centre Commun de Mesure de l'Université des Sciences et Techniques de Lille." The crystallographic data are given in Table I. Lattice parameters and their standard deviations were determined by least-squares refinement of the setting angles of 25 carefully centered reflections. The densities were not measured: from comparison with the cubic, elpasolite phase Cs_2KBiCl_6, we assumed the existence of eight formula units per unit cell. The parameters of these compounds suggest that they are isomorphic.

The crystal structures were solved by the heavy atom method: Patterson synthesis, successive Fourier difference maps and least-squares refinements in the centrosymmetric space group *C*2/*c*. Refinement of the atomic parameters and isotropic thermal factors for all of the atoms led to the values $R = 0.166$ and $R = 0.152$ for Cs_3BiCl_6 and CsK_2BiCl_6, respectively. At this step, absorption corrections were applied using the method described recently by Walker and Stuart (*8*), by means of a program written by one of us (*9*). The knowledge of crystal dimensions and linear absorption coefficients is not required in this method, which proved to be very useful with badly shaped crystals containing heavy atoms. Following absorption corrections, R indexes dropped to 0.098 for Cs_3BiCl_6 and 0.073 for CsK_2BiCl_6; use of anisotropic thermal coefficients led to final R values of 0.069 (Rw = 0.083) for Cs_3BiCl_6, and $R = 0.044$ (Rw = 0.049) for CsK_2BiCl_6 (with $w = 1$ for all reflections). In the last cycle, the maximum parameter shift was lower than 10^{-3} times the corresponding estimated standard deviation. The final Fourier difference maps were featureless. The scattering factors for Cs^+, K^+, Bi^{3+}, and Cl^- were taken from Cromer and Waber (*10*), with anomalous dispersion corrections according to Cromer and Libermann (*11*). The positional parameters are listed in Table II.

TABLE I

EXPERIMENTAL DATA AND STRUCTURE REFINEMENT PARAMETERS FOR Cs_3BiCl_6 AND CsK_2BiCl_6

Formula	Cs_3BiCl_6	CsK_2BiCl_6
System	Monoclinic	Monoclinic
Space group	*C*2/*c*	*C*2/*c*
Lattice parameters	a = 27.017 (17)	a = 25.653 (13)
measured at 294	b = 8.252 (8)	b = 7.799 (5)
K with 25 *hkl*	c = 13.121 (10)	c = 12.874 (9)
$5° < \theta < 12°$	β = 99.70 (11)	β = 99.24 (8)
Volumes (Å^3)	V = 2883	V = 2542
Multiplicity	Z = 8	Z = 8
Calculated density	ρ = 3.78 g · cm^{-3}	ρ = 3.31 g · cm^{-3}
Data collection technique	w-2θ scan Philips PW 1100 diffractometer Mo$K\bar{\alpha}$ radiation λ = 0.7107 Å	
Scan speed	0.06° s^{-1}	0.03° s^{-1}
Scan width	1.2°	1.2°
Standard reflections	$\bar{6}22$, $6\bar{2}\bar{2}$, $62\bar{2}$	$\bar{3}11$, $60\bar{2}$, $51\bar{1}$
Periodicity	60 mn	120 mn
Recorded reflections	8964 (within a $2 < \theta < 24°$ sphere)	4680 (within a $2 < \theta < 25°$ half sphere)
Observed reflections ($I > 3I$)	6128	3727
Independent reflections	1706	2008
R merging factor	0.114	0.050
Absorption coefficient	μ = 203 cm^{-1}	μ = 179 cm^{-1}
Absorption correction	Walker and Stuart method (DIFABS)	
Refined parameters	93	93
Reliability factors	R = 0.069 Rw = 0.083 (w = 1)	R = 0.044 Rw = 0.049 (w = 1)

TABLE II

ATOMIC COORDINATES AND ANISOTROPIC THERMAL PARAMETERS[a,b]

	Atom	x	y	z	U_{11}	U_{22}	U_{33}	U_{12}	U_{13}	U_{23}	B_{eq}
Cs_3BiCl_6	Bi(1)	¼	¼	½	29(3)	26(1)	23(1)	−3(1)	7(2)	2(1)	2.0
	Bi(2)	0	7835(2)	¼	25(3)	26(1)	20(1)	0	7(2)	0	1.9
	Cs(1)	496(1)	7444(4)	9317(2)	57(3)	82(2)	53(2)	15(1)	19(2)	24(2)	5.0
	Cs(2)	1614(1)	8133(3)	2982(2)	36(3)	38(1)	52(2)	−1(1)	12(2)	−3(1)	3.3
	Cs(3)	3462(1)	1863(3)	8546(2)	39(3)	33(1)	41(2)	3(1)	5(2)	−3(1)	3.0
	Cl(1)	2492(3)	3890(11)	6871(7)	43(3)	40(5)	35(5)	−2(4)	10(3)	−4(4)	3.1
	Cl(2)	3235(2)	4548(13)	4639(8)	72(7)	54(6)	40(6)	−29(6)	23(5)	−3(5)	4.4
	Cl(3)	3269(4)	549(14)	5813(8)	65(7)	56(6)	46(6)	26(6)	9(5)	12(5)	4.4
	Cl(4)	572(4)	5536(12)	1815(8)	51(7)	46(6)	47(6)	9(4)	16(5)	−6(5)	3.8
	Cl(5)	−583(4)	7739(16)	641(7)	51(7)	90(8)	27(5)	3(6)	3(3)	−2(5)	4.4
	Cl(6)	576(4)	10263(12)	1928(9)	39(7)	47(6)	58(7)	1(4)	16(5)	17(5)	3.8
CsK_2BiCl_6	Bi(1)	¼	¼	½	26(1)	29(1)	29(1)	−2(1)	6(1)	5(1)	2.21
	Bi(2)	0	7786(1)	¼	26(1)	22(1)	22(1)	0	8(1)	0	1.84
	Cs	512(1)	7363(1)	9307(1)	42(1)	52(1)	43(1)	5(1)	8(1)	11(1)	3.61
	K(1)	1622(2)	8129(5)	3004(3)	39(3)	36(2)	72(2)	5(1)	8(2)	4(2)	3.9
	K(2)	3432(2)	1906(5)	8756(3)	45(3)	35(2)	63(2)	11(1)	18(2)	−3(1)	3.8
	Cl(1)	2503(2)	3906(6)	6939(6)	62(3)	47(2)	34(2)	−9(1)	15(2)	−7(2)	3.8
	Cl(2)	3275(2)	4665(7)	4708(4)	52(3)	63(3)	75(3)	−6(2)	10(3)	25(2)	5.0
	Cl(3)	3267(2)	274(7)	5771(5)	58(3)	62(3)	87(4)	5(2)	8(3)	35(3)	5.4
	Cl(4)	643(2)	5405(6)	1845(3)	55(3)	46(2)	43(2)	5(1)	8(1)	−8(2)	3.8
	Cl(5)	−589(2)	7653(6)	600(3)	42(3)	61(3)	31(2)	1(1)	2(1)	−1(2)	3.5
	Cl(6)	642(2)	10310(5)	1991(4)	39(3)	36(3)	56(2)	−11(1)	18(1)	13(2)	3.4

[a] Atomic parameters $\times 10^4$ and vibrational coefficients $\times 10^3$.

[b] The anisotropic thermal parameters are relative to $T = \exp[-2\pi^2(h^2a^{*2}U_{11} + k^2b^{*2}U_{22} + l^2c^{*2}U_{33} + 2hka^*b^*U_{12} + 2hla^*c^*U_{13} + 2klb^*c^*U_{23})]$.

The noncentrosymmetric $C2$ space group was also checked, but no significant improvement was observed in the R values. Furthermore, anisotropic thermal coefficients for two of the Cl atoms became negative, indicating correlation effects; thus both structures are described in the $C2/c$ space group.

The higher R value for Cs_3BiCl_6, compared with CsK_2BiCl_6, is likely due to the poor quality of the crystal, as mentioned previously. Furthermore, since superstructure reflections have been neglected, atomic coordinates for Cs_3BiCl_6 describe a "mean structure" (probably phase II) and not the actual one (phase I). The importance of this superstructure must not be underestimated: since the mean structure (phase II) is centrosymmetric, the remanent polarization at $T < T_1$ (phase I) on one hand, and the dielectric anomalies at T_1 on the other hand (*6*), may be related to the existence and the disappearance of this superstructure, respectively.

Atomic parameters are very close in these structures (Table II), confirming that these phases are isostructural. Thermal motion factors for K and Cs in CsK_2BiCl_6 (Table II) were refined to reasonable values, in agreement with their ordered distribution.

Structural Results

The characteristic bond lengths and angles are reported in Table III. As in a number of chlorides, the $6s^2$ nonbonding pair of

TABLE III

INTRAANIONIC DISTANCES (Å) AND ANGLES (°) WITH ESDS IN Cs_3BiCl_6 and CsK_2BiCl_6

	Cs_3BiCl_6	CsK_2BiCl_6
Bi(1)–Cl(1)	2.713(9)	2.725(4)
Bi(1)–Cl(2)	2.709(8)	2.681(5)
Bi(1)–Cl(3)	2.702(11)	2.691(5)
Bi(2)–Cl(4)	2.695(11)	2.707(5)
Bi(2)–Cl(5)	2.672(9)	2.663(4)
Bi(2)–Cl(6)	2.719(11)	2.714(5)
	⟨2.702⟩	⟨2.697⟩
Cl(1)–Bi(1)–Cl(2)	90.7(5)	89.0(3)
Cl(1)–Bi(1)–Cl(3)	91.0(5)	91.6(3)
Cl(2)–Bi(1)–Cl(3)	84.4(5)	86.7(3)
Cl(4)–Bi(2)–Cl(5)	87.6(5)	88.4(2)
Cl(4)–Bi(2)–Cl(6)	92.3(5)	89.9(2)
Cl(5)–Bi(2)–Cl(6)	92.7(6)	94.8(2)

Bi^{3+} does not induce a significant distortion of the octahedral symmetry in $BiCl_6^{3-}$: the angles are close to 90° and the Bi–Cl distances range from 2.672(11) to 2.719(11) Å and from 2.663(5) to 2.725(5) Å in Cs_3BiCl_6 and CsK_2BiCl_6, respectively. These values are in fair agreement with the accurate distance of 2.676(2) Å recently calculated in $Cs_2NaBiCl_6$ (*12*).

The anionic framework is built up of two kinds of $BiCl_6$ octahedra exhibiting different orientations (Fig. 2). The coordination polyhedra of Cl atoms around the alkaline cations are quite irregular in both structures: in Cs_3BiCl_6, Cs(1) is surrounded by 11Cl atoms (as Cs in CsK_2BiCl_6), while Cs(2) and Cs(3) are surrounded by 8 Cl atoms (as K(1) and K(2) in CsK_2BiCl_6), (Table IV). The Cs · · · Cl distances range from 3.37(1) to 4.28(1) Å in Cs_3BiCl_6, and from 3.508(6) to 4.119(5) Å in CsK_2BiCl_6 (compared with 3.820(2) Å in $Cs_2NaBiCl_6$(12)); the K · · · Cl distances range from 2.996(7) to 4.006(7) Å.

It is worthwhile to notice that, starting from the ideal cubic phase Cs_2KBiCl_6, the same deformation occurs when substituting K by Cs (Cs_3BiCl_6) or Cs by K (CsK_2BiCl_6). This behavior may be due to the fact that these crystal compositions are "equidistant" from the cubic compound.

According to the solubility diagram (13), Cs_3BiCl_6 can also be prepared from an hydrochloric solution (14% in mass) saturated with a $3CsCl/1BiCl_3$ mixture at 25°C. Indeed, slow evaporation provided colorless platelet-shaped single crystals. An X-ray diffraction study disclosed an orthorhombic symmetry, space group *Pnma*. This result suggested that this phase is very likely iso-

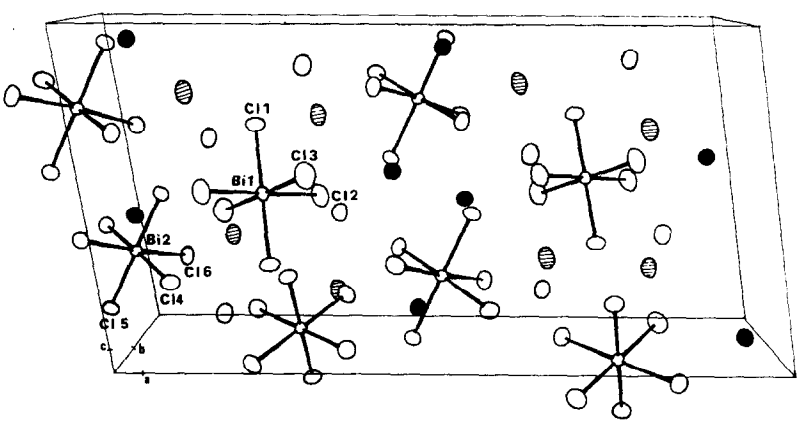

FIG. 2. Perspective drawing of CsK_2BiCl_6 (monoclinic C2/c) showing the numbering scheme. Thermal ellipsoids are drawn at the 50% probability level.

TABLE IV

CATIONIC SURROUNDINGS WITH ESDS IN Cs_3BiCl_6 AND CsK_2BiCl_6 (Å)

	Cs_3BiCl_6			CsK_2BiCl_6
Cs(1)–Cl(4)	1/001	3.61(1)	Cs	3.573(4)
Cs(1)–Cl(6)	2/021	3.61(1)		3.642(5)
Cs(1)–Cl(5)	1/001	3.64(1)		3.508(6)
Cs(1)–Cl(6)	4/020	3.70(1)		3.552(5)
Cs(1)–Cl(3)	7/001	3.71(1)		3.546(6)
Cs(1)–Cl(2)	7/001	3.88(1)		3.640(5)
Cs(1)–Cl(4)	2/011	3.89(1)		3.772(5)
Cs(1)–Cl(5)	2/021	3.98(1)		3.893(5)
Cs(1)–Cl(6)	1/001	4.12(1)		4.119(5)
Cs(1)–Cl(4)	4/010	4.13(1)		3.894(5)
Cs(1)–Cl(5)	2/011	4.28(1)		3.918(5)
Cs(2)–Cl(6)	1/000	3.40(1)	K(1)	3.140(6)
Cs(2)–Cl(3)	6/001	3.42(1)		3.077(7)
Cs(2)–Cl(1)	4/01$\bar{1}$	3.42(1)		3.241(7)
Cs(2)–Cl(1)	6/011	3.43(1)		3.215(7)
Cs(2)–Cl(5)	3/000	3.58(1)		3.452(7)
Cs(2)–Cl(2)	6/011	3.63(1)		3.385(6)
Cs(2)–Cl(4)	1/000	3.66(1)		3.442(6)
Cs(2)–Cl(2)	7/000	3.72(1)		3.741(7)
Cs(3)–Cl(4)	6/001	3.37(1)	K(2)	3.173(7)
Cs(3)–Cl(2)	4/010	3.39(1)		2.996(7)
Cs(3)–Cl(5)	5/0$\bar{1}$1	3.51(3)		3.220(6)
Cs(3)–Cl(1)	7/0$\bar{1}$1	3.53(1)		3.367(6)
Cs(3)–Cl(1)	1/000	3.54(1)		3.434(6)
Cs(3)–Cl(6)	6/011	3.65(1)		3.466(7)
Cs(3)–Cl(3)	4/000	3.69(1)		3.186(8)
Cs(3)–Cl(3)	1/000	3.70(1)		4.006(7)

Coding of equivalent positions

1	x, y, z	5	$\frac{1}{2}+x, \frac{1}{2}+y, z$
2	$\bar{x}, \bar{y}, \bar{z}$	6	$\frac{1}{2}-x, \frac{1}{2}-y, \bar{z}$
3	$\bar{x}, y, \frac{1}{2}-z$	7	$\frac{1}{2}-x, \frac{1}{2}+y, \frac{1}{2}-z$
4	$x, \bar{y}, \frac{1}{2}+z$	8	$\frac{1}{2}+x, \frac{1}{2}-y, \frac{1}{2}+z$

Cl(4) 1/001 means that Cl(4) is in position 1 translated by 1c

structural with Rb_3BiBr_6 (*14*), and constitutes another allotropic form which does not appear in the Cs_3BiCl_6–K_3BiCl_6 equilibrium diagram (*4*). Annealing of this phase in a sealed quartz tube at 350°C (60°C below the phase II ⇄ phase III transition (Fig. 1)) resulted in a room-temperature X-ray powder spectrum identical to the Cs_3BiCl_6 monoclinic pattern. This orthorhombic form will be hereafter labeled phase IV. Its unit-cell parameters are $a = 26.593(9)$, $b = 8.290(4)$, $c = 13.129(7)$ Å, $V = 2894$ Å^3 ($Z = 8$) in the *Pmcn* space group (after *bca* permutation to facilitate comparison with the monoclinic phase II (Table I)). The structure of this phase was not redetermined and the atomic coordinates of Rb_3BiBr_6 were used in the representation (Fig. 3) (*15*).

The two structures, monoclinic (phase II) and orthorhombic (phase IV), essentially differ by the **a** parameter, which implies a modification in the relative disposition of $BiCl_6$ octahedra in these two cells with identical contents. The point groups 2/*m* (phase II) and *mmm* (phase IV) are subgroups of that of the prototype cubic phase *m*3*m*. A relation between all of these phases can be found by computing the Bi · · · Bi distances and Bi–Bi–Bi angles) from the atomic coordinates. Possible transformation matrices can be written as

$$\begin{pmatrix} a_c \\ b_c \\ c_c \end{pmatrix} = \begin{pmatrix} \frac{1}{4} & 1 & -\frac{1}{4} \\ \frac{1}{4} & 0 & \frac{3}{4} \\ \frac{1}{4} & -1 & -\frac{1}{4} \end{pmatrix} \begin{pmatrix} a_m \\ b_m \\ c_m \end{pmatrix} \quad \text{and}$$

$$\begin{pmatrix} a_c \\ b_c \\ c_c \end{pmatrix} = \begin{pmatrix} \frac{1}{4} & 1 & -\frac{1}{3} \\ \frac{1}{4} & 0 & \frac{2}{3} \\ \frac{1}{4} & -1 & -\frac{1}{3} \end{pmatrix} \begin{pmatrix} a_o \\ b_o \\ c_o \end{pmatrix}$$

where subscripts c, m, and o referring evidently to cubic, monoclinic and orthorhombic cells. Applying these operations, the pseudo-cubic cells are for Cs_3BiCl_6 (*C*2/*c*): $a = 11.687$, $b = 10.691$, $c = 11.290$, $\alpha = 88.30$, $\beta = 91.91$, $\gamma = 86.32$ (average $a = 11.313$ Å); for CsK_2BiCl_6 (*C*2/*c*): $a = 11.067$, $b = 10.702$, $c = 10.748$, $\alpha = 89.13$, $\beta = 91.28$, $\gamma = 87.48$ (average $a = 10.839$ Å); for Cs_3BiCl_6 (*Pmcn*): $a = 11.498$, $b = 11.028$, $c = 11.452$, $\alpha = 87.35$, $\beta = 92.51$, $\gamma = 87.12$ (average $a = 11.326$ Å). These values must be compared to the parameter $a = 11.086(5)$ Å of cubic Cs_2KBiCl_6 (*5*). The inverse matrices, which describe the cubic →

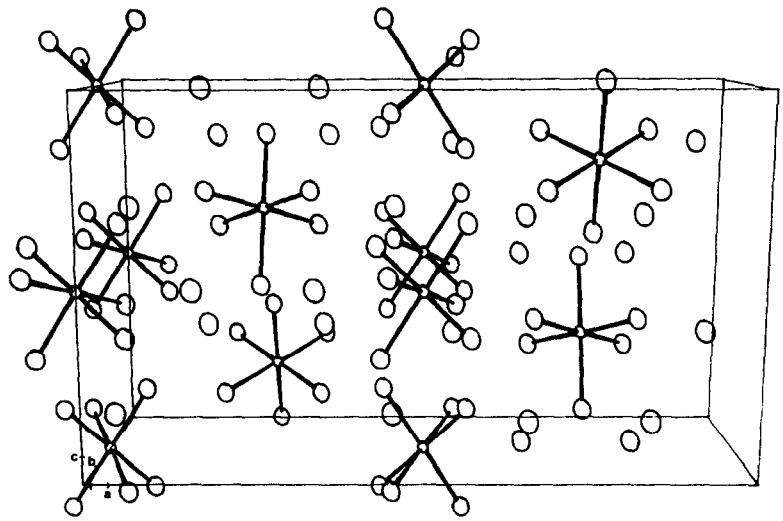

FIG. 3. Perspective drawing of Cs_3BiCl_6 (orthorhombic *Pmcn*).

monoclinic and the cubic → orthorhombic transformations, can be written as

$$\begin{pmatrix} a_m \\ b_m \\ c_m \end{pmatrix} = \begin{pmatrix} \frac{3}{2} & 1 & \frac{3}{2} \\ \frac{1}{2} & 0 & -\frac{1}{2} \\ -\frac{1}{2} & 1 & -\frac{1}{2} \end{pmatrix} \begin{pmatrix} a_c \\ b_c \\ c_c \end{pmatrix} \quad \text{and}$$

$$\begin{pmatrix} a_o \\ b_o \\ c_o \end{pmatrix} = \begin{pmatrix} \frac{4}{3} & \frac{4}{3} & \frac{4}{3} \\ \frac{1}{2} & 0 & -\frac{1}{2} \\ -\frac{1}{2} & 1 & -\frac{1}{2} \end{pmatrix} \begin{pmatrix} a_c \\ b_c \\ c_c \end{pmatrix}.$$

These vectorial relations are illustrated in Fig. 4. With an ideal cubic cell parameter of 11.320 Å for Cs_3BiCl_6, we obtain a_m = 26.547, b_m = 8.004, c_m = 13.863 Å, β = 100.02°, and a_o = 26.141, b_o = 8.004, c_o = 13.863 Å. The differences from the experimental values arise from the extensive deformations produced by the substitution of one K by one Cs atom (or vice versa). Moreover, these relationships are only based on the Bi · · · Bi distances and do not take into account the rotations of the $BiCl_6$ octahedra, as compared to their primitive orientation in the cubic phase: clearly, this fact must be more precisely defined to understand the relationships between all of the phases.

Relations between Monoclinic, Orthorhombic, and Cubic Phases of Cs_3BiCl_6

Structures of halides of formulas $A_xB_yX_{3x}$ (ABX_3, A_2BX_6, and $A_3B_2X_9$) are generally described as resulting from compact stacking of AX_3 layers, the B cations occupying totally or partially the octahedral sites defined by X atoms (*16*). Among the compounds containing isolated BX_6 anions, in elpasolite Cs_2KBiCl_6 cubic $Fm3m$, all of the octahedral sites are alternatively occupied

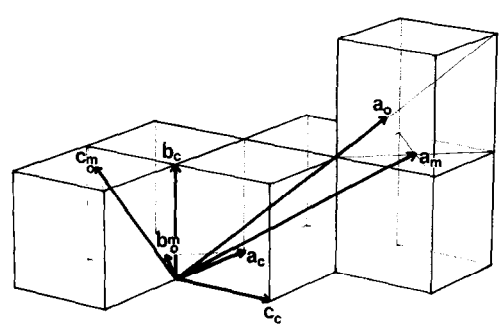

FIG. 4. Orthorhombic and monoclinic cells derived from the prototype cubic cell.

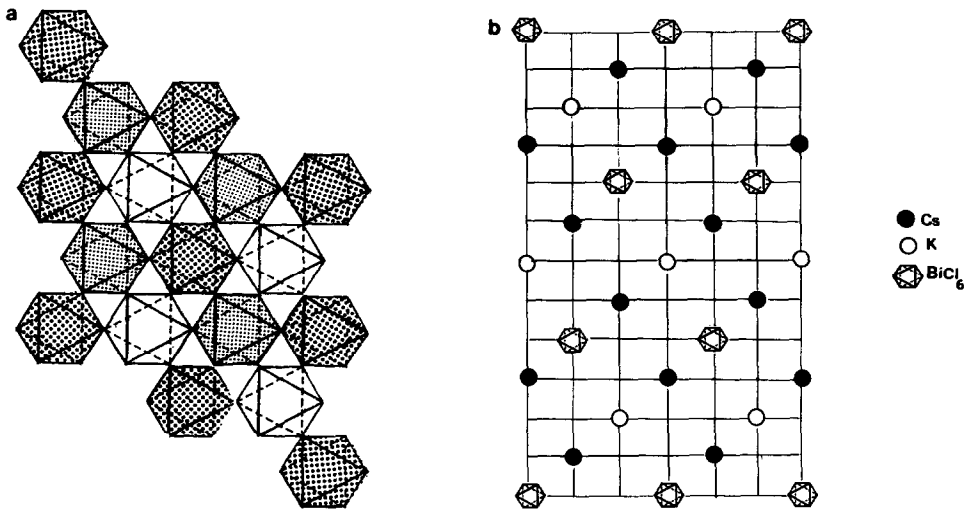

FIG. 5. Cubic Cs_2KBiCl_6 structure: (a) projection of the "three $BiCl_6$ layers"; (b) diagrammatic elevation.

by Bi^{3+} and K^+ cations, whereas in K_2PtCl_6 half of the octahedral sites are occupied by Pt atoms. This last compound is also described as an antifluorine structure in which the nearly spherical complexe ions $PtCl_6^{2-}$ define "octahedral" and "tetrahedral" holes which can accommodate K^+ cations (*16*). The first description assumes the existence of AX_3 layers which are planar, or very nearly so. The second one, considering the BX_6 octahedra as entities, can describe structures built of isolated octahedra, whatever their respective orientations, that is to say, even when the AX_3 layers are no longer definable.

In this manner, the cubic *Fm3m* prototype phase (Cs_2KBiCl_6) can be described as a compact stacking of "layers of close-packed octahedra ($BiCl_6$)," according to the *ABC* sequence characteristic of fcc structures, in the direction of a body diagonal of the cube (Figs. 5a and b). In such "layers," all of the octahedra have a threefold axis parallel to the stacking direction.

If we consider the monoclinic and orthorhombic phases, their common crystallographic axes **b** and **c** are both contained in a (111) type plane of the cubic prototype phase (Fig. 4). Projections of these two structures along the direction normal to the (**b**, **c**) plane, which is the stacking direction of the octahedra layers, show the existence of two types of layers: (i) layers similar to those observed in the cubic phase, containing only octahedra viewed along a threefold axis (which will be labeled *OIII* hereafter) (Figs. 6a and 7a); (ii) layers containing octahedra viewed along a twofold axis (labeled *OII*) (Figs. 6b and 7b), and oriented in two manners in the layer plane. These octahedra are obtained by a 45° rotation of an *OIII* octahedron around two of its three fourfold axes (Fig. 8). Lack of the third possible orientation is probably due to steric hindrance. Although the *OII* layers are identical in phases II and IV, the *OIII* layers are slightly different. The rows of octahedra parallel to **c** are all identical in phase II and also identical to the rows of the cubic phase (Figs. 5a and 6a). However, phase IV presents an alternance of two types of rows, differing by a rotation of the octahedra by about 60° (Fig. 7a). The structures of phases II (C2/*c*) and IV (*Pmcn*) can then be

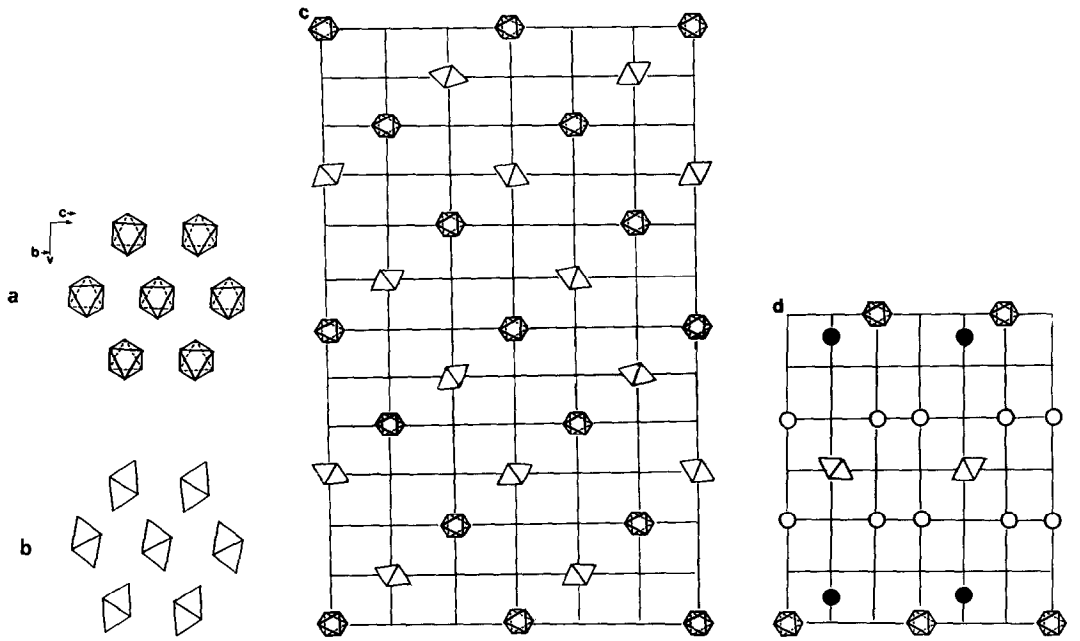

FIG. 6. $BiCl_6$ layers in monoclinic Cs_3BiCl_6 and CsK_2BiCl_6: (a) *OIII* layer; (b) *OII* layer; (c) diagrammatic elevation of monoclinic CsK_2BiCl_6, 12-layer sequence of $BiCl_6$ layers; (d) cationic disposition between 3 $BiCl_6$ layers.

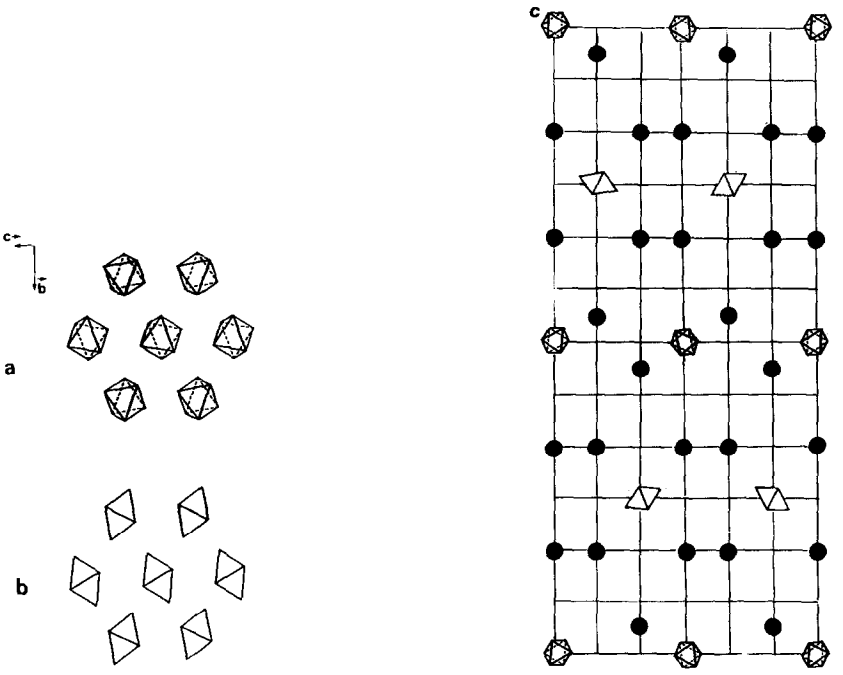

FIG. 7. Orthorhombic Cs_3BiCl_6 structure: (a) *OIII* layer; (b) *OII* layer; (c) 4-layer sequence of $BiCl_6$ layers.

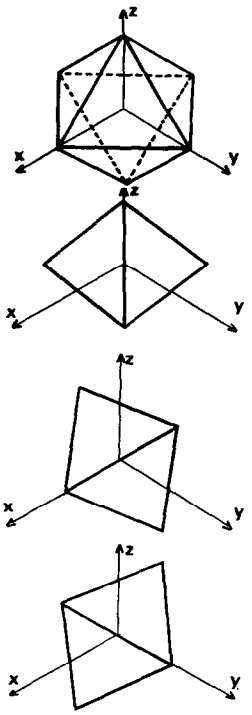

FIG. 8. 45° rotation of an octahedron around its four-fold axes.

described by an alternation of layers *OII* and *OIII* stacked along the direction normal to the (**b**, **c**) plane. There is a succession of four layers in the case of phase IV (Fig. 7c) and of twelve layers in phase II (Fig. 6c). This representation in "layers of close-packed octahedra" displays the filiation between the phases stable at room temperature and the prototype phase stable at high temperature.

Despite the different stacking sequences (3, 4, or 12 layers), the alkaline cation sites are identical in all structures: they fill the octahedral and tetrahedral holes created between the $BiCl_6$ octahedra. For example, in phase II, Cs(1) is in a tetrahedral site constituted by three *OIII* and one *OII* (Fig. 9a); Cs(3) is also in a tetrahedral hole, but built with three *OII* and one *OIII* (Fig. 9b), whereas Cs(2) lies in an octahedral hole (Fig. 9c). The different orientations of these octahedra explain the variations in the number of coordinating Cl atoms about cations occupying similar sites: 11 around Cs(1), but only 8 around Cs(3) (Table IV).

Metric relations between phases II and IV of Cs_3BiCl_6, phase II′ (CsK_2BiCl_6) and the cubic phase (Cs_2KBiCl_6) are summarized in Table V, using the pseudohexagonal cells, where the **c** axis has been chosen the stacking direction in order to make the comparison easier.

The structure of phase III, which is intermediate between phase II stable at ambient temperature and the prototype phase, is unknown at present. It is therefore impossible to describe the complete transition sequences. Nevertheless, by comparison of Figs. 5b and 6c, it is obvious that the relative disposition of the octahedra layers remains unchanged, but some *OII* must be

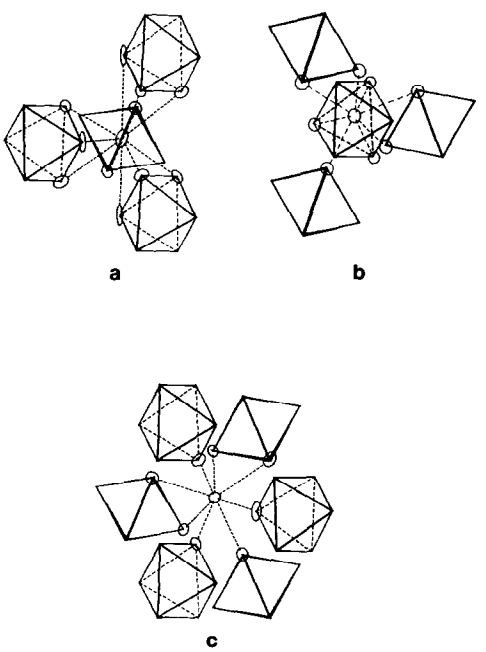

FIG. 9. Cationic surroundings in monoclinic Cs_3BiCl_6: (a) three *OIII* and one *OII* around Cs(1); (b) three *OII* and one *OIII* around Cs(3); (c) three *OIII* and three *OII* around Cs(2).

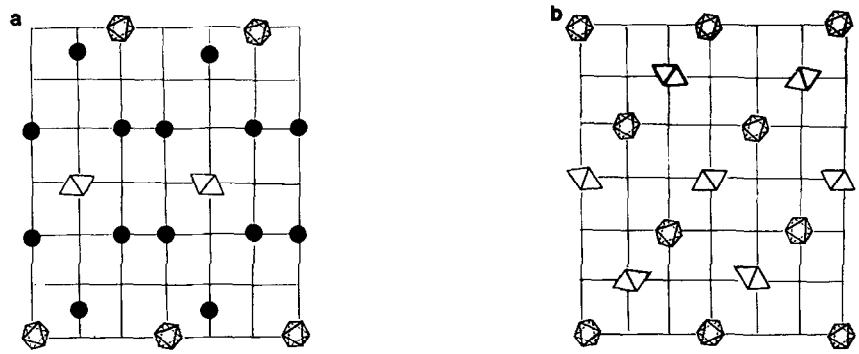

FIG. 10. Monoclinic K_3MoCl_6 structure: (a) cationic disposition between 3 $MoCl_6$ layers; (b) 6-layer sequence of $MoCl_6$ layers.

rotated to *OIII*; displacive phase transitions would thus be expected.

Generalization to A_3MX_6, A_2BMX_6, and A_2MX_6 Compounds

It is possible to compare the Cs_3BiCl_6 phases II and IV crystal structures with other compounds of similar formulas. For example, K_3MoCl_6 has been described (*17*) in a monoclinic cell $P2_1/a$ (a = 12.160, b = 7.534, c = 12.731 Å, β = 108.66°). A projection of this structure along the normal to the (**a**, **b**) plane reveals an alternation of *OIII* and *OII* layers with a six-layer sequence (Figs. 10a and b).

Cryolite Na_3AlF_6 has the monoclinic symmetry $P2_{1/n}$ (*18*) (a = 5.46, b = 5.61, c = 7.80 Å, β = 90.11°). The similarity of this cell to that of cubic elpasolite (*19*) implies that [2**a** + **c**] is the stacking direction for a three-layer disposition; in each layer, the AlF_6 octahedra exhibit a "rotational distortion," as termed by (*20*) (Fig. 11).

We have gathered in Table VI some significant examples of compounds with general formulas A_3MX_6, A_2BMX_6, and A_2MX_6, where the anionic network consists of isolated MX_6 octahedra, as in the compounds that we have studied. These examples are illustrated in Fig. 12. In Table VI, we have

TABLE V

PSEUDO-HEXAGONAL CELLS IN Cs–K–Bi MIXED CHLORIDES: PARAMETERS (Å AND °), L NUMBER OF $BiCl_6$ LAYERS, AND d INTERLAYER DISTANCE

	a	b	c	γ(°)	L	d
Cs_2KBiCl_6 (*Fm3m*)	15.678[a]	15.678[a]	19.20	120	3	6.40
Cs_3BiCl_6 (*Pmcn*)	15.58	15.53	26.593	122.3	4	6.65
Cs_3BiCl_6 (*C2/c*)	16.50	15.50	78.894	122.2	12	6.66
CsK_2BiCl_6 (*C2/c*)	15.60	15.05	75.96	121.2	12	6.33

[a] Doubled parameters.

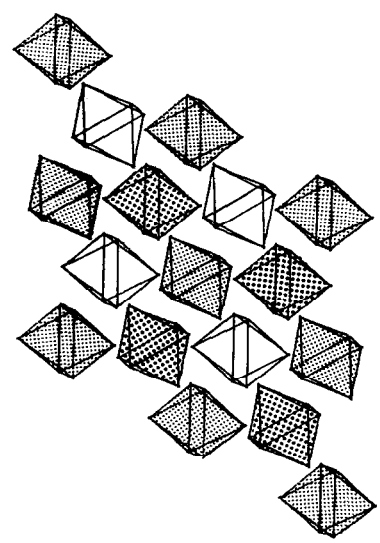

FIG. 11. Orientation of the AlF_6 octahedra in cryolite Na_3AlF_6.

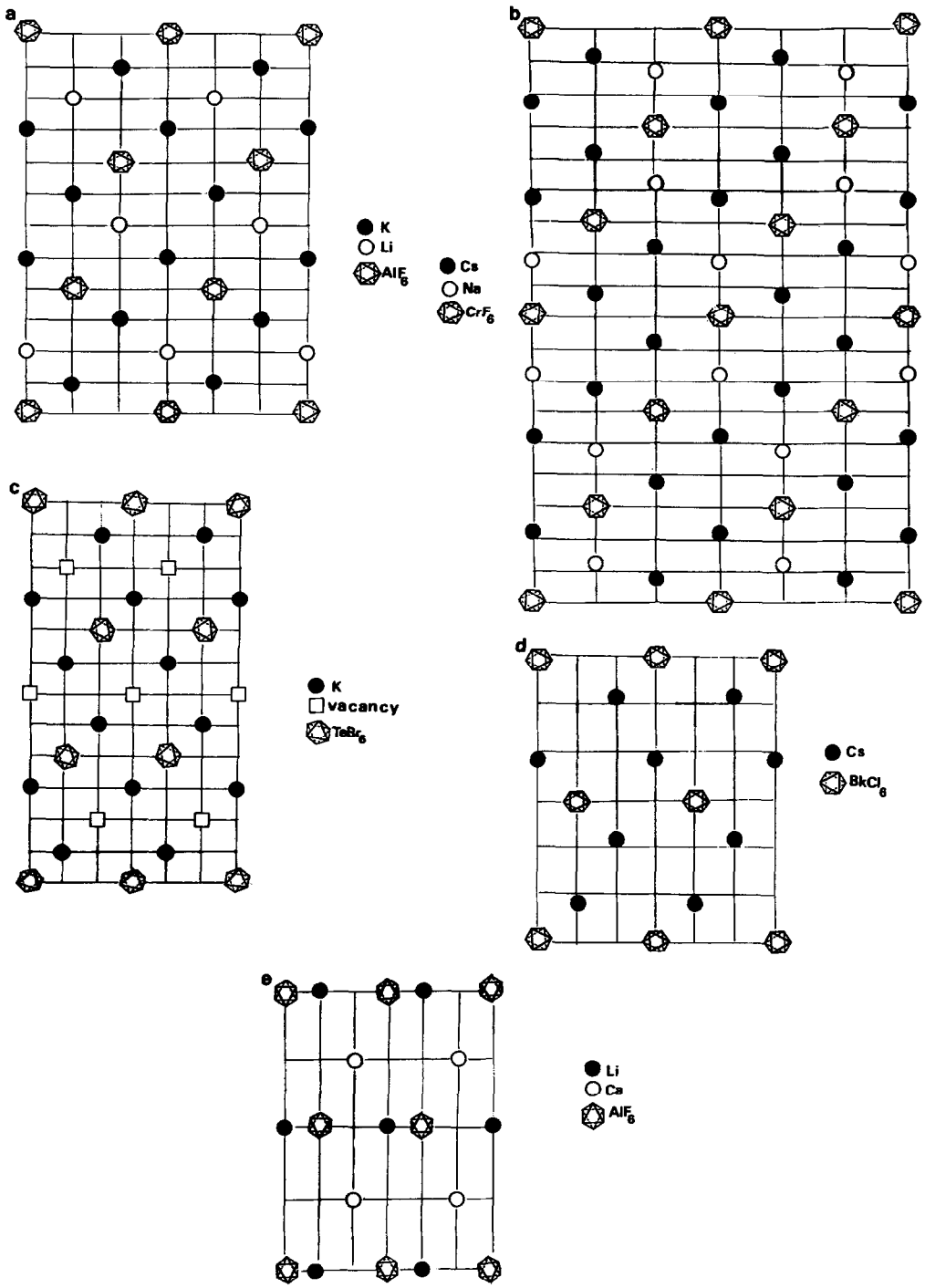

FIG. 12. (a) 3-layer sequence and cationic disposition in K_2LiAlF_6. (b) 6-layer sequence and cationic disposition in Cs_2NaCrF_6. (c) 3-layer sequence and cationic disposition in K_2TeBr_6. (d) 2-layer sequence and cationic disposition in Cs_2BkCl_6. (e) 2-layer sequence and cationic disposition in $LiCaAlF_6$.

TABLE VI

Compound	Space group	Number of layers	Sites occupied		References
			Octahedral	Tetrahedral	
Cs_2KBiCl_6	$Fm3m$	3*L*	1K	2Cs	(*3*)
K_2LiAlF_6	$P3m1$	3*L*	1Li/3,2K/6	2Li/3,4K/6	(*21, 22*)
Cs_2NaCrF_6	$R\bar{3}m$	6*L*	1Cs	1Cs,1Na	(*23*)
CsK_2BiCl_6	$C2/c$	12*L*	1K	1K,1Cs	([a])
$(NH_4)_3FeF_6$	$Fm3m$	3*L*	$1NH_4$	$2NH_4$	(*24*)
Na_3AlF_6	$P2_1/n$	3*L*	1Na	2Na	(*18*)
Ca_3UO_6	$P2_1$	3*L*	1Ca	2Ca	(*25*)
Cs_3BiCl_6	$Pnma$	4*L*	1Cs	2Cs	([a], *14*)
K_3MoCl_6	$P2_1/a$	6*L*	1K	2K	(*17*)
Cs_3BiCl_6	$C2/c$	12*L*	1Cs	2Cs	([a])
K_2PtCl_6	$Fm3m$	3*L*		2K	(*26*)
K_2TeBr_6	$P2_1/n$	3*L*		2K	(*27*)
Cs_2BkCl_6	$P6_3mc$	2*L*	1Cs	1Cs	(*28*)
$LiCaAlF_6$[b]	$P\bar{3}1c$	2*L*	1Ca	"1Li"	(*29*)

[a] This work.

[b] A borderline case in this representation as the Li^+ cation and the central Al atom of the AlF_6 octahedron are located at the same altitude (Fig. 12e).

voluntarily omitted all the structures resulting from slight distortions of a cubic $Fm3m$ phase, which are evidently three-layer structures: this is the case of all of the tetragonal phases in which the c/a ratio is close to 1 or 1.414 (*30–39*). It must be pointed out that, in each family the most symmetrical phases pertain to the $m3m$ point group, and that all of the others belong to subgroups of $m3m$ (except Cs_2BkCl_6).

Some compounds containing only Li^+ or Na^+ cations cannot be described by using the notion of "layers of close-packed octahedra." The small size of these cations enables them to occupy centers of X_6 octahedra and therefore, it is no longer necessary to use sites between the MX_6 layers. This is the case for Li_3AlF_6 ($Pna2_1$) (*40*), Li_3VF_6 ($C2/c$) (*41*), Na_2ScF_6 ($P321$) (*42*), and Li_2MoF_6 ($P42_12$) (*43*). Nevertheless, in most cases it is possible in this way to describe, and rationally explain, many crystal structures which seem at first sight to be completely unrelated.

Acknowledgments

The authors are indebted to the referees of the journal for their enlightening suggestions.

References

1. R. Schwartz, S. Watkins, C. O'Connor, and R. Carlin, *J. Chem. Soc. Faraday Trans. 2* **72,** 565 (1976).
2. G. Meyer and E. Dietzel, *Rev. Chim. Min.* **16,** 189 (1979).
3. B. V. Beznosikov and S. V. Misyul, *Sov. Phys. Crystallogr.* **23,** 346 (1978).
4. P. Barbier, M. Drache, G. Mairesse, and J. Ravez, *Ferroelectrics* **55,** 113 (1984).
5. P. Barbier, M. Drache, G. Mairesse, and J. Ravez, *J. Solid State Chem.* **42,** 130 (1982).
6. R. Von Der Mühl, J. Ravez, P. Hagenmuller, P. Barbier, M. Drache, and G. Mairesse, *Solid State Commun.* **43,** 797 (1982).
7. L. R. Morss and W. R. Robinson, *Acta Crystallogr. Sect. B* **28,** 653 (1972).
8. N. Walker and D. Stuart, *Acta Crystallogr. Sect. A* **39,** 158 (1983).
9. G. Nowogrocki, unpublished program, 1985.
10. D. T. Cromer and J. T. Waber, *Acta Crystallogr.* **18,** 104 (1965).

11. D. T. CROMER AND D. LIBERMAN, *J. Chem. Phys.* **53,** 1891 (1970).

12. F. PELLE, B. BLANZAT, AND B. CHEVALIER, *Solid State Commun.* **49,** 1089 (1984).

13. S. B. STEPINA, I. V. VLASOVA, N. P. SOKOLOVA, AND V. E. PLYUSHCHEV. *Russ. J. Inorg. Chem.* **13,** 1473 (1968).

14. F. LAZARINI, *Acta Crystallogr.* **B34,** 2288 (1978).

15. C. K. JOHNSON, Ortep Report ORNL-3794, Oak Ridge National Laboratory, Tennessee, 1965.

16. A. F. WELLS, "Structural Inorganic Chemistry," 3rd ed., Clarendon Press, Oxford, 1962.

17. Z. AMILIUS, B. VAN LAAR, AND H. M. RIETVELD, *Acta Crystallogr. Sect. B* **25,** 400 (1969).

18. NARAY-SZABO AND K. SASVARI, *Z. Kristall.* **99,** 27 (1938).

19. E. G. STEWARD AND H. P. ROOKSBY, *Acta Crystallogr.* **6,** 49 (1953).

20. K. S. ALEKSANDROV AND S. V. MISYUL, *Sov. Phys. Crystallogr.* **26,** 612 (1981).

21. H. G. F. WINKLER, *Acta Crystallogr.* **7,** 33 (1954).

22. A. TRESSAUD, J. DARRIET, P. LAGASSIE, J. GRANNEC, AND P. HAGENMULLER, *Mat. Res. Bull.* **19,** 983 (1984).

23. D. BADEL AND R. HAEGELE, *J. Solid State Chem.* **18,** 39 (1976).

24. V. CAGLIOTTI AND G. GIACOMELLO, *Naturwiss.* **26,** 317 (1938).

25. B. O. LOOPSTRA AND H. M. RIETVELD, *Acta Crystallogr. Sect. B* **25,** 787 (1969).

26. F. J. EWING AND L. PAULING, *Z. Kristall.* **68,** 223 (1928).

27. I. D. BROWN, *Can. J. Chem.* **42,** 2758 (1964).

28. L. R. MORSS AND J. FUGER, *Inorg. Chem.* **8,** 1433 (1969).

29. W. VIEBAHN, *Z. Anorg. Allg. Chem.* **386,** 335 (1971).

30. H. BODE AND E. VOSS, *Z. Anorg. Allg. Chem.* **290,** 1 (1957).

31. G. BLASSE, *J. Inorg. Nucl. Chem.* **27,** 993 (1965).

32. G. MEYER AND H. C. GAEBELL, *Z. Naturforsch.* **33,** 1476 (1978).

33. G. MEYER AND E. DIETZEL, *Rev. Chim. Min.* **16,** 189 (1979).

34. W. ABRIEL, *Mat. Res. Bull.* **17,** 1341 (1982); **18,** 1419 (1983); **19,** 313 (1984).

35. J. SETTER AND R. HOPPE, *Z. Anorg. Allg. Chem.* **423,** 125 (1976).

36. W. ABRIEL AND J. IHRINGER, *J. Solid State Chem.* **52,** 274 (1984).

37. A. TRESSAUD, J. PORTIER, S. SHEARER-TURRELL, J. L. DUPIN, AND P. HAGENMULLER, *J. Inorg. Nucl. Chem.* **32,** 2179 (1970).

38. R. NEVALD, F. W. FOSS, O. V. NIELSEN, H. D. AMBERGER, AND R. D. FISCHER, *Solid State Commun.* **32,** 1223 (1979).

39. S. KAIROUN, J. M. DANCE, J. GRANNEC, G. DEMAZEAU, AND A. TRESSAUD, *Rev. Chim. Min.* **20,** 871 (1983).

40. J. H. BURNS, A. C. TENNISSEN, AND G. D. BRUNTON, *Acta Crystallogr. Sect. B* **24,** 225 (1968).

41. W. MASSA, *Z. Kristall.* **153,** 201 (1980).

42. A. ZALKIN, J. D. FORRESTER, AND D. H. TEMPLETON, *Acta Crystallogr.* **17,** 1408 (1964).

43. G. BRUNTON, *Mat. Res. Bull.* **6,** 555 (1971).